METTL3 suppresses anlotinib sensitivity by regulating m 6 A modification of FGFR3 in oral squamous cell carcinoma

Jie Chen
First Affiliated Hospital of Sun Yat-sen University
Shuai Li
College of Stomatology, Guangxi Medical University, China
Zhexun Huang
Stomatological Hospital, Southern Medical University,China
Congyuan Cao
First Affiliated Hospital of Sun Yat-sen University
Anxun Wang
First Affiliated Hospital of Sun Yat-sen University
Qianting He (heqt3@mail.sysu.edu.cn)
First Affiliated Hospital of Sun Yat-sen University

Research Article

Keywords: OSCC, Anlotinib, METTL3, FGFR3, TKI, m6A methylation

Posted Date: May 25th, 2022

DOI: https://doi.org/10.21203/rs.3.rs-1664250/v1

Abstract

Purpose: N6-methyladenosine (m^6A) is an abundant nucleotide modification in mRNA, but there were few studies of its role in the cancer drug sensitivity and resistance. Anlotinib has been proved to have effective antitumor effects in oral squamous cell carcinoma (OSCC) in our previous study. Here, we sought to investigate the treatment target of anlotinib and the function and mechanisms of m^6A modification in regulating anlotinib effect in OSCC.

Methods: Anlotinib treatment in a dose-dependent manner, western blotting, qRT-PCR and cell lost-of function assays were used to study the treatment target of anlotinib in OSCC. RNA m^6A dot blot assays the m^6A MeRIP-seq and MeRIP-qPCR, RNA and protein stability assays were used to explore the m^6A modification of the treatment target of anlotinib. Cell lost-of function assays after METTL3 depletion were conducted to investigate the effect of m^6A modification level on the therapeutic effect of anlotinib in OSCC. Patient-derived tumor xenograft (PDX) models and immunohistochemistry staining were performed to study the relationship of METTL3 and antitumor sensitivity of anlotinib in vivo.

Results: Anlotinib targeted FGFR3 in the treatment of OSCC and inhibited tumor cell proliferation and promoted apoptosis by inactivating the FGFR3/AKT/mTOR signaling pathway. METTL3 was identified to target and modify FGFR3 m^6A methylation and then decrease mRNA stability. METTL3 expression level was related to the anlotinib sensitivity in OSCC cells in vitro and METTL3 knockdown promoted anlotinib sensitivity of OSCC cells by inhibited the FGFR3 expression. PDX models samples furthermore showed that METTL3 and FGFR3 levels are tightly correlated with the anlotinib efficacy in OSCC.

Conclusion: In summary, our work revealed that FGFR3 was served as the treatment target of anlotinib and METTL3-mediated FGFR3 m^6A modification played a critical function in the anlotinib sensitivity in OSCC.

1. Introduction

Oral squamous cell carcinoma (OSCC) is the most common malignant tumor of the oral cavity and prone to local recurrence and metastasis[1,2]. To date, palliative drug therapy is an important treatment for patients with advanced, recurrent and metastatic OSCC[2], including traditional cytotoxic chemotherapy (Cisplatin, 5-FU and Paclitaxel), molecular targeted therapy (Cetuximab, Nimotuzumab and Sorafenib) and immunotherapy (Pembrolizumab and Nivolumab)[3–6]. However, tumors heterogeneity and the existence of drug resistance had been proved to limited the therapeutic effect of drug therapy effect. Thus, elucidation of mechanisms underlying the sensitivity and resistance to these drugs is needed to improve response in OSCC patient[6–8].

Anlotinib is a multi-target tyrosine kinase inhibitor (TKI) that can efficiently and selectively inhibit tyrosine kinase activity and then inhibit phosphorylation of downstream related proteins[9–11], such as vascular endothelial cell growth factor receptor 1, 2, 3 (VEGFR1, VEGFR2, VEGFR3), stem cell growth factor receptor (c-Kit), platelet-derived growth factor receptor beta (PDGFRβ) and fibroblast growth factor receptor (FGFR)1–4. Multiple studies have shown that anlotinib has anti-angiogenic effect and direct killing effect on a variety of tumor cells[11–15]. Our previous study also found that anlotinib monotherapy exerted favorable anticancer

activity and manageable toxicities in patients with recurrent and metastatic OSCC[16]. However, the reported anlotinib insensitiveness and resistance imped its anti-tumor effectiveness[17,18].

Cancer therapeutic sensitivity is an intricated phenomenon affected by multiple mechanisms[19–22], including altered expression of drug influx/efflux transporters, altered role of DNA repair and impairment of apoptosis, and altered epigenomics influencing upstream or downstream effectors, et al. As a dynamic and reversible internal modification of RNA, N6-methyladenosine (m^6A) methylation has been frequently reported promoting the tumor growth and metastasis in human cancers[23–28]. Targeting key regulators of m^6A modification may be a potential cancer treatment target[23]. We previously studied that RNA m^6A modification enzyme methyltransferase-like 3 (METTL3) promoted OSCC proliferation and metastasis through B cell-specific Moloney murine leukemia virus insertion site 1 (BMI1) m^6A methylation[29]. To date, many studies had found that METTL3 regulate drug resistance in human cancers. Jin et al[30] found that RNA m^6A modification enzyme methyltransferase-like 3 (METTL3) induced RNA m^6A modification upregulating ATP binding cassette subfamily G member 2 (ABCG2) transcripts and regulated ABCG2-dependent multidrug resistance in non-small cell lung cancer. Uddin et al[31] found that METTL3 depletion suppressed the expression of mutant p53 and sensitized colorectal cells to doxorubicin. METTL3 upregulates the expression of ubiquitin-conjugating enzyme E2B (UBE2B), a critical DNA damage repair enzyme, leading to drug resistance to 5-FU, cisplatin and gemcitabine[32,33].

To date, the exact target and the underline mechanism of anlotinib in OSCC had not been sufficient elucidated. In this study, we aimed to explore the exact target of anlotinib in OSCC and explore the role of m^6A modification in anlotinib sensitivity of OSCC. Functional studies revealed that anlotinib targeted FGFR3 in the treatment of OSCC in virto. m^6A-RNA immunoprecipitation and sequencing (MeRIP-seq), MeRIP-qPCR, and RNA and protein stability assays revealed that METTL3 modifying FGFR3 mRNA m^6A modification and decreasing FGFR3 mRNA stability. METTL3 knockdown promoted anlotinib sensitivity of OSCC cells by increasing FGFR3 expression, and METTL3 and FGFR3 levels were tightly correlated with the anlotinib efficacy in OSCC.

2. Materials And Methods

2.1. Cell culture and transfection

Human normal oral epithelial keratinocytes (HOK) cells were purchased from ScienCell. Human umbilical cord veins cells (HUVECs), UM1, SCC9, SCC15 and SCC25 were purchased from the ATCC. All the cells were cultured in Dulbecco's modified Eagle's medium/F12 (Gibco, New York, USA) supplemented with 10% fetal bovine serum (FBS; Gibco) and 1% penicillin-streptomycin, and incubated 5% CO_2 at 37°C. Anlotinib dihydrochloride was kindly provided by the Chia Tai Tianqing Pharmaceutical Group Co. Ltd. (Nanjing, China). Anlotinib powder was dissolved in normal saline.

Lentivirus vectors containing METTL3 short hairpin RNA (shRNA) were purchased from OBiOc (Shanghai, China). Small interfering RNAs (siRNAs) (RiboBio, Guangzhou, China) targeting FGFR3 were designed to knockdown FGFR3 in OSCC. The indicated two shRNA and three siFGFR3 sequences are listed in Table S1.

2.2. Cell proliferation

The cells (5×10^3) were seeded in 96-well plates and treated with indicated concentrations of anlotinib for 24h. Cell viability was measured using Cell Counting Kit-8 (CCK-8) (Dojindo, Japan) following the manufacturer's instructions and calculated using the formula: $([OD_t - OD_b] / [OD_c - OD_b]) \times 100\%$ (OD: optical density, t: treated sample, c: control sample, b: blank sample). IC_{50} values were calculated using GraphPad Prism software (San Diego, CA, USA).

2.3. Cell apoptosis assay

Cell apoptosis assays was conducted with Annexin V-FITC/PI Apoptosis Assay Kit (MultiSciences, Hangzhou, China) according to the manufacturer's protocol. After treatment with anlotinib for 24 h, the fixed and stained cells were analyzed by flow cytometry using CytoFLEX (Beckman Coulter, Brea, USA). Flowjo software of 7.6 version (FLOWJO LLC, Ashland, USA) was employed for data analysis.

2.4. Western Blotting

Total protein were harvested by lysing in radioimmunoprecipitation assay (RIPA) buffer with proteinase inhibitor cocktail and conditionally adding phosphatase inhibitors (Sangon Biotech, Shanghai, China). The protein samples were then mixed with 5 × loading buffer and denatured at 95℃ for 5 min. The aliquots of protein were subjected to 10% sodium dodecyl sulfate–polyacrylamide gel electrophoresis (SDS-PAGE) and electrotransferred to the polyvinylidene fluoride (PVDF) membrane. After blocking with 5% skimmed milk and incubation with primary antibodies overnight at 4℃, Tris-buffered saline with Tween 20 (TBST)-diluted secondary antibody was applied. Then, the protein antibody complexes were detected using the enhanced chemiluminescence (ECL) method with Tanon 5200 Multi intelligent imaging system.

2.5. Quantitative real-time PCR (qRT-PCR)

Total RNAs were extracted with TRIzol™ Reagent (Invitrogen, Carlsbad, USA) following the manufacturer's instruction. Reverse-transcription was conducted with 1μg RNA using PrimeScript RT Master Mix kit (Takara, Japan). Then, quantitative PCR (qPCR) was carried out with TB Green Premix Ex Taq II kit (Takara, Japan) in StepOnePlusTM Real-Time PCR Instrument (Thermo Fisher Scientific). The relative mRNA expression levels were calculated using β-Action as the internal control. All primer sequences are listed in Table S1

2.6. MeRIP-seq and MeRIP-qPCR

The m^6A MeRIP-seq and MeRIP-qPCR were performed according to the published procedure with slight modifications[29,34]. Briefly, total RNA was fragmented using ZnCl2 and incubated with anti-m^6A polyclonal antibody (Synaptic Systems, 202003) or anti-IgG antibody (Abcam, ab150080) for 2 h at 4°C and then treated with protein A/G magnetic beads (Thermo Fisher Scientific; 88802) at 4°C for an additional 2 h to obtain immunoprecipitated RNA fragments. The bound RNA was purified and then used for sequencing library construction and qRT-PCR. The library was sequenced with the Illumina Next-Seq 500 sequencer and analyzed as previously described. Methylated sites on RNAs (peaks) were identified with MACS software.

2.7. RNA m^6A Dot Blot Assays

A total of 2 μg RNA was denatured at 95°C for 3 min and crosslinked to the Hybond-N + membrane in a crosslinker twice using 1,200 μJ for 50s. The membrane was incubated with m^6A antibody, followed by secondary antibody. The intensity of dot blot signal was detected using ECL with Tanon 5200 Multi intelligent imaging system. Then the membrane was stained with 0.02% Methylene blue (Sigma-Aldrich, St. Louis, USA), followed by the scanning to indicate the total content of input RNA.

2.8. RNA and Protein Stability Assays

To evaluate the RNA and protein stability, RNA and protein decay assay was conducted. For RNA decay assay, indicated OSCC cells were treated with actinomycin D (ActD, 5 μg/mL) for 0, 3, and 6 h. Total RNA was then isolated and subject to qRT-PCR to quantify the relative abundance of FGFR3 mRNA (relative to 0 h). For protein decay assay, indicated OSCC cells were treated with cycloheximide (CHX, 100 μg/mL) (Sigma-Aldrich) at 0, 2, 4, and 8 h. Then the expression of FGFR3 was measured via western blotting.

2.9. Patient-derived tumor xenograft (PDX) models and Immunohistochemistry staining (IHC)

The OSCC sample were from the OSCC PDX models which had been established in previously described[16]. In brief, eight patients' samples were used to establish the PDX models and the PDX models were treated with 3 mg/kg anlotinib or normal saline (oral administration, once a day). The tumor growth inhibition (TGI) rate was calculated as (1-(Tn-T0)/(Cn-C0)) × 100% and presented in our previous study[16].

Tissue slides from PDX models were routinely deparaffinized and rehydrated. After quenching of endogenous peroxidase and antigen retrieval, the slides were blocked in 5% BSA for 30 min, followed by incubating with primary antibodies against METTL3 (1:100) and FGFR3 (1:100) overnight at 4℃. Then secondary antibodies and SABC were applied with SABC-POD (rabbit IgG) kit (BOSTER, Wuhan, China). The color was developed with 3,3'-diaminobenzidine (DAB) kit (BOSTER) and counterstained with hematoxylin.

2.10. Statistical analyses

The data are presented as the mean ± standard deviation (SD). Differences between the two groups were determined using the student's *t*-tests. Statistical analyses were carried out using SPSS (version 25.0; IBM Corporation, Armonk, NY, USA). $P < 0.05$ were considered statistically significant. All experiments were performed in triplicate.

3. Results

3.1. Anlotinib targets FGFR3 and inhibits FGFR3 phosphorylation in the treatment of OSCC

To explore the possible anlotinib targets, firstly, we detected the mRNA expression levels of *VEGFR1-3, FGFR1-4, PDGFRβ* and *C-KIT* genes in four OSCC cell lines by qRT-PCR. We found that HUVECs mainly expressed *FGFR1 and VEGFR2* mRNA (Fig. 1A and Table 1). However, HOK and OSCC cells expressed low mRNA levels of *VEGFR1-3, PDGFRβ* and *C-KIT* genes, but with high mRNA levels of *FGFR1-4* genes (Fig. 1A and Table 1). Furthermore, four OSCC cell lines mainly expressed *FGFR3* mRNA among *FGFR1-4* (Fig. 1A and Table 1). We

further evaluated the protein levels of the above genes by western blotting and found that VEGFR1, c-Kit and PDGFRβ were barely detected, VEGFR2 and VEGFR3 protein basically not expressed in OSCC cells (Fig. 1B). Meanwhile, FGFR3 protein had the highest expression levels among FGFR1-4 protein in OSCC cells (Fig. 1B). Although the FGFR3 protein levels were not obviously changed after anlotinib treatment, we found the phosphorylation levels of FGFR3 were significantly reduced in the anlotinib group in a dose-dependent manner in OSCC cells compared with the non-anlotinib group (Fig. 1C and Supplementary Fig. 1). These above results implied that FGFR3 may act as the anlotinib target in OSCC cells.

Table 1
Relative mRNA expression of therapeutic target of Anlotinib in OSCC cell lines

Cell line	VEFGR1	VEFGR2	VEFGR3	PDGFRβ	FGFR1	FGFR2	FGFR3	FGFR4	c-KIT
HUVECs	1.000	3.896	0.065	0.034	29.590	0.002	0.073	0.008	0.667
HOK	0.335	0.255	0.226	0.401	106.328	2.551	1.861	0.628	0.709
SCC9	0.323	0.032	0.011	0.695	2.211	3.605	11.951	3.400	0.149
SCC15	0.095	0.426	0.074	0.740	1.648	7.160	12.289	3.144	0.005
SCC25	0.025	0.004	0.042	0.806	1.722	9.049	13.947	3.048	0.000
UM1	0.007	0.003	0.009	0.247	1.589	0.710	13.122	3.571	0.005
The VEGFR1 expression level of HUVEC was defined as 1.									

3.2. FGFR3 expression level affects antitumor activity of anlotinib in OSCC

To further examine the role of FGFR3 in anlotinib-induced antitumor effects in OSCC, three different sequences of siFGFR3 were used to transfer into the SCC9 and SCC15 cells, and the siRNA with the highest silencing efficacy (siFGFR3-3) was selected for subsequent experiments (Fig. 2A). As shown in Fig. 2B-D, anlotinib induced proliferation inhibition (Fig. 2B) and apoptosis (Fig. 2C) in SCC9 and SCC25 in a dose-dependent manner. The phosphorylation of FGFR3, AKT and mTOR was decreased after anlotinib treatment (Fig. 2D). The ability of proliferation inhibition and apoptosis stimulation effects of anlotinib was significantly decreased after knockdown FGFR3 in OSCC cells, moreover, the phosphorylation levels of FGFR3, AKT and mTOR were slightly increased after knockdown FGFR3, suggesting that lower FGFR3 expression levels led to less anlotinib sensitivity of OSCC. Recombinant human FGF-2 (rhFGF-2, 20 ng/mL), which can stimulate autophosphorylation of FGFR3 and the phosphorylation levels of AKT and mTOR, also significantly diminished the ability of proliferation inhibition and apoptosis stimulation effects of anlotinib in OSCC cells (Fig. 2B-C and Supplementary Fig. 2). After anlotinib treatment, the phosphorylation levels of FGFR3, AKT and mTOR were decreased in rhFGF-2-treated plus anlotinib group. These changes caused subsequent corresponding changes of downstream apoptosis proteins, including BAX and BCL-2 (Fig. 2D).

Overall, these results suggested that anlotinib targeted and inhibited FGFR3 phosphorylation levels and then affected the subsequent AKT/mTOR phosphorylation to cause apoptosis of OSCC cells.

METTL3 regulates FGFR3 mRNA m ^{6}A modification and decreases FGFR3 mRNA stability

To investigate how METTL3 regulate FGFR3 in OSCC cells, firstly, we knocked down METTL3 in SCC9 and SCC25 cells and found that the m^6A levels were significantly decreased in METTL3-knockdown group by dot-blot analysis (Fig. 3A). We then analyzed the data of m^6A MeRIP-seq from our previous study[29] and found that the m^6A peaks of FGFR3 was enriched near the 3'UTR regions (Fig. 3B). MeRIP-qPCR assay also showed that FGFR3 m^6A modification was significantly decreased after METTL3 knockdown in SCC9 and SCC25 cells (Fig. 3C). Western blotting showed that METTL3 knockdown increased FGFR3 protein and mRNA expression levels (Fig. 3D). These data suggested that METTL3 might regulate FGFR3 expression at the post-transcriptional level.

Moreover, we compared FGFR3 mRNA and protein stability in METTL3-knockdown group with control cells by actinomycin D and cycloheximide assay. We found that the stability of FGFR3 mRNA level was remarkably increased in METTL3-knockdown cells compared with control cells, but without changing the degradation rate of FGFR3 protein level (Fig. 4E and F). The results manifested that FGFR3 mRNA m^6A modification by METTL3 could accelerate its degradation.

METTL3 are inversely associated with anlotinib sensitivity in OSCC cells

To investigate the role of METTL3 in anlotinib treated OSCC cells, we explored the correlation between anlotinib sensitivity (IC50 values) and METTL3 expression level in OSCC cell lines. Four OSCC cell lines (SCC9, SCC15, SCC25 and UM1) were treated with anlotinib (Fig. 4A), and the expression of endogenous METTL3 was assessed by qRT-PCR and western blotting in OSCC cell lines (Fig. 4B-C). Strong correlation between IC50 and METTL3 expression level was identified in OSCC cells. The OSCC cells with higher METTL3 expression were less sensitive to anlotinib (higher IC50 values) (Table 2). METTL3 knockdown in OSCC cells sensitized the inhibitory effects of anlotinib in OSCC cells. The IC50 value was decreased and the apoptosis was increased after anlotinib treatment in METTL3 knockdown OSCC cells (Fig. 4D-E and Supplementary Fig. 3).

Table 2
Correlation analysis of IC50 and METTL3 expression of different OSCC cells

Cell line	SCC9	SCC15	SCC25	UM1	Pearson
IC50	5.157	3.315	3.524	6.420	
METTL3 mRNA level	1.778	1.528	1.715	1.959	0.967
METTL3 protein level*	0.780	0.838	0.722	0.868	0.926

*The radio between the gray value of METTL3 protein and GAPDH protein. Pearson correlation coefficient was METTL3 expression level relative to IC50.

METTL3 affects the FGFR3 expression and antitumor efficacy of anlotinib in PDX models

To verify the relationship of METTL3, FGFR3 and antitumor sensitivity of anlotinib in vivo, we explored the expression level of METTL3 and FGFR3 of tumor tissues from eight previously established OSCC PDX models[16]. After 30 days of anlotinib treatment, the TGI rate of anlotinib was evaluated to measure the antitumor sensitivity of anlotinib of OSCC PDX. TGI values in eight PDX models were 95.90 (#005), 92.28 (#010), 78.07 (#022), 92.85 (#024), 92.89 (#030), 92.89 (#032), 88.25 (#034) and 89.18% (#040).

Histopathological examination (H&E) and IHC assay were used to detect the expression level of METTL3/FGFR3 in the control group of each PDX models (Fig. 5A-C). As shown in Fig. 5D, the expression level of METTL3/FGFR3 had significant correlationship with TGI rate in PDX models. PDX models with the lower expression level of METTL3 or the higher expression level of FGFR3 displayed more sensitive to anlotinib treatment with higher TGI rate (Fig. 5D). Meanwhile, the expression levels of METTL3 and FGFR were significantly negatively correlated in each PDX sample (Fig. 5D).

4. Discussion

In recent decades, despite the application of various treatment modalities for OSCC, the five-year overall survival rate of OSCC remains at 50%[35]. As a new, orally administered multi-target TKI, anlotinib exhibits excellent antitumor effects for several types of cancer[12,36–38]. Our previously study[16] also confirmed that anlotinib exerted potent antiproliferation capability and induced apoptosis in OSCC cells, and favorable anticancer activity and manageable toxicities in patients with recurrent and metastatic OSCC. Until now tremendous studies had been performed to investigate th mechanism of anlotinib in the treatment of human cancers. Previous studies had found that PI3K/AKT/ mTOR signaling pathway and downstream apoptosis pathway were typical mechanism in anlotinib treatment[13]. Song et al[13] found that anlotinib mainly inhibited the phosphorylation level of VEGFR2 and then affected PIK3/AKT signal activation in intrahepatic cholangiocarcinoma (ICC). Yang et al[39] suggested that anlotinib suppressed cell proliferation and angiogenesis via inhibition of VEGFR-2/AKT and FGFR, PDGFRβ and their downstream signaling ERK in colorectal cancer. In this study, we further confirmed that the antitumor effect of anlotinib was conducted by targeting FGFR3 and inhibiting the phosphorylation level of FGFR3, and subsequent inhibition of the AKT/mTOR and apoptosis signaling pathway in OSCC. Taken together, these results suggested that anlotinib may involved in the FGFR3/AKT/mTOR signaling pathway in the therapeutic of OSCC.

As the most pervasive internal modification of mRNA, m^6A modification is installed by a methyltransferase complex (e.g., METTL3-METTL14), erased by demethylases (e.g., FTO and ALKBH5), and can be recognized by readers (e.g., YTHDF1-3, IGF2BP1-3)[29]. Studies have proved that mRNA m^6A modification can affect RNA splicing, RNA stability, RNA translation efficiency, RNA secondary structure and RNA subcellular localization[23]. Tremendous studies have shown that METTL3 promotes the tumor growth, metastasis, and drug resistance in human cancers[26–28, 40,41]. Recently, Yan et al[42] identified the dynamic m^6A methylome as an additional epigenetic driver for reversible TKI tolerance. Ianniello et al[43] also found that downregulation of METTL3 and METTL14 overcame the resistance of chronic myeloid leukemia cells to the TKI imatinib mesylate (imatinib) through regulating ribosome levels and translation. Sa et al[44] demonstrated that insulin-like growth factor 2 mRNA-binding protein 2 (IGF2BP2)-dependent ERBB2 signaling activation contributes to acquired resistance to TKI of radioiodine-refractory papillary thyroid cancer. In the present study, we identified the function of m^6A methylation in regulating anlotinib sensitivity of OSCC, providing a mechanistic paradigm for drug sensitivity in cancer. Cell lost-of-functional assays revealed that FGFR3 act as the anlotinib target in OSCC cells. Our MeRIP-seq and MeRIP-qPCR results demonstrated that FGFR3 was selectively m^6A modified in OSCC. Depletion of METTL3 decreased FGFR3 m^6A methylation and mRNA stability, and promoted anlotinib sensitivity of OSCC cells. OSCC PDX models verified that METTL3 and FGFR3 levels were tightly correlated

with the anlotinib efficacy in the treatment of OSCC, and the expression levels of METTL3 and FGFR were significantly negatively correlated in each PDX sample. Thus, METTL3-mediated m^6A modification played a critical function in the anlotinib sensitivity of OSCC.

5. Conclusions

Anlotinib targeted and inhibited FGFR3 phosphorylation in the treatment of OSCC. METTL3 modified FGFR3 m^6A methylation and decrease its stability which attenuate the effect of anlotinib. The METTL3/m^6A axis could serve as a biomarker to predict response of the OSCC patients to the anlotinib treatment.

Declarations

Ethical Approval and Consent to participate: The animal experiments were approved by the Ethical Committee of the First Affiliated Hospital, Sun Yat-Sen University (No. [2019] 069)

Consent for publication: Not applicable.

Availability of supporting data: All data generated or analyzed during this study are included in this article [and its additional files].

Competing interests The authors have declared that no conflict of interest exists.

Funding This study was supported by National Natural Science Foundation of China (82173041 and 82002871).

Authors' contributions A.W. and Q.H. conceived of, designed, and supervised the study; J.C., S.L. and Z.H. wrote the main manuscript text and prepared figure 1-5; C.C. checked and wrote part of the manuscript; All authors reviewed the manuscript.

Acknowledgements Not applicable.

Authors' information Affiliations the First Affiliated Hospital, Sun Yat-Sen University, Guangzhou.

References

1. L.Q.M. Chow, Head and Neck Cancer. N Engl. J. Med. (2020). doi:10.1056/NEJMra1715715
2. D.G. Pfister, S. Spencer, D. Adelstein, D. Adkins, Y. Anzai, D.M. Brizel, J.Y. Bruce, P.M. Busse, J.J. Caudell, A.J. Cmelak, A.D. Colevas, D.W. Eisele, M. Fenton, R.L. Foote, T. Galloway, M.L. Gillison, R.I. Haddad, W.L. Hicks, Y.J. Hitchcock, A. Jimeno, D. Leizman, E. Maghami, L.K. Mell, B.B. Mittal, H.A. Pinto, J.A. Ridge, J.W. Rocco, C.P. Rodriguez, J.P. Shah, R.S. Weber, G. Weinstein, M. Witek, F. Worden, S.S. Yom, W. Zhen, J.L. Burns, S.D. Darlow, Head and Neck Cancers, Version 2.2020, NCCN Clinical Practice Guidelines in Oncology. J. Natl. Compr. Canc Netw. (2020). doi:10.6004/jnccn.2020.0031
3. M. Taberna, M. Oliva, R. Mesía, Cetuximab-Containing Combinations in Locally Advanced and Recurrent or Metastatic Head and Neck Squamous Cell Carcinoma. Front. Oncol. (2019).

doi:10.3389/fonc.2019.00383

4. R.L. Ferris, Immunology and Immunotherapy of Head and Neck Cancer. J. Clin. Oncol. (2015). doi:10.1200/jco.2015.61.1509
5. I. Micaily, J. Johnson, A. Argiris, An update on angiogenesis targeting in head and neck squamous cell carcinoma. Cancers Head Neck (2020). doi:10.1186/s41199-020-00051-9
6. E.E.W. Cohen, R.B. Bell, C.B. Bifulco, B. Burtness, M.L. Gillison, K.J. Harrington, Q.T. Le, N.Y. Lee, R. Leidner, R.L. Lewis, L. Licitra, H. Mehanna, L.K. Mell, A. Raben, A.G. Sikora, R. Uppaluri, F. Whitworth, D.P. Zandberg, R.L. Ferris, The Society for Immunotherapy of Cancer consensus statement on immunotherapy for the treatment of squamous cell carcinoma of the head and neck (HNSCC). J. for. Immunother Cancer (2019). doi:10.1186/s40425-019-0662-5
7. W. Qiang, Y. Dai, X. Xing, X. Sun, Identification and validation of a prognostic signature and combination drug therapy for immunotherapy of head and neck squamous cell carcinoma. Comput. Struct. Biotechnol. J. (2021). doi:10.1016/j.csbj.2021.01.046
8. B. Patel, N.F. Saba, Current Aspects and Future Considerations of EGFR Inhibition in Locally Advanced and Recurrent Metastatic Squamous Cell Carcinoma of the Head and Neck. Cancers (2021). doi:10.3390/cancers13143545
9. Y.Y. Syed, Anlotinib: First Global Approval. Drugs (2018). doi:10.1007/s40265-018-0939-x
10. G. Shen, F. Zheng, D. Ren, F. Du, Q. Dong, Z. Wang, F. Zhao, R. Ahmad, J. Zhao, Anlotinib: a novel multi-targeting tyrosine kinase inhibitor in clinical development. J. Hematol. Oncol. (2018). doi:10.1186/s13045-018-0664-7
11. C. Xie, X. Wan, H. Quan, M. Zheng, L. Fu, Y. Li, L. Lou, Preclinical characterization of anlotinib, a highly potent and selective vascular endothelial growth factor receptor-2 inhibitor. Cancer Sci. (2018). doi:10.1111/cas.13536
12. G. Wang, M. Sun, Y. Jiang, T. Zhang, W. Sun, H. Wang, F. Yin, Z. Wang, W. Sang, J. Xu, M. Mao, D. Zuo, Z. Zhou, C. Wang, Z. Fu, Z. Wang, Z. Duan, Y. Hua, Z. Cai, Anlotinib, a novel small molecular tyrosine kinase inhibitor, suppresses growth and metastasis via dual blockade of VEGFR2 and MET in osteosarcoma. Int. J. Cancer (2019). doi:10.1002/ijc.32180
13. F. Song, B. Hu, J.W. Cheng, Y.F. Sun, K.Q. Zhou, P.X. Wang, W. Guo, J. Zhou, J. Fan, Z. Chen, X.R. Yang, Anlotinib suppresses tumor progression via blocking the VEGFR2/PI3K/AKT cascade in intrahepatic cholangiocarcinoma. Cell. Death Dis. (2020). doi:10.1038/s41419-020-02749-7
14. B. Lin, X. Song, D. Yang, D. Bai, Y. Yao, N. Lu, Anlotinib inhibits angiogenesis via suppressing the activation of VEGFR2, PDGFRβ and FGFR1. Gene (2018). doi:10.1016/j.gene.2018.02.026
15. Z. Deng, W. Liao, W. Wei, G. Zhong, C. He, H. Zhang, Q. Liu, X. Xu, J. Liang, Z. Liu, Anlotinib as a promising inhibitor on tumor growth of oral squamous cell carcinoma through cell apoptosis and mitotic catastrophe. Cancer Cell. Int. (2021). doi:10.1186/s12935-020-01721-x
16. Z. Huang, Q. Su, W. Li, H. Ren, H. Huang, A. Wang, Suppressed mitochondrial respiration via NOX5-mediated redox imbalance contributes to the antitumor activity of anlotinib in oral squamous cell carcinoma. J. Genet. Genomics (2021). doi:10.1016/j.jgg.2021.06.014

17. J. Lu, W. Xu, J. Qian, S. Wang, B. Zhang, L. Zhang, R. Qiao, M. Hu, Y. Zhao, X. Zhao, B. Han, Transcriptome profiling analysis reveals that CXCL2 is involved in anlotinib resistance in human lung cancer cells. BMC Med. Genomics (2019). doi:10.1186/s12920-019-0482-y
18. G. Gu, C. Hu, K. Hui, T. Chen, H. Zhang, X. Jiang, NEAT 1 knockdown enhances the sensitivity of human non-small-cell lung cancer cells to anlotinib. Aging (Albany NY) (2021). doi:10.18632/aging.203004
19. R.K. Vadlapatla, A.D. Vadlapudi, D. Pal, A.K. Mitra, Mechanisms of drug resistance in cancer chemotherapy: coordinated role and regulation of efflux transporters and metabolizing enzymes. Curr. Pharm. Des. (2013). doi:10.2174/13816128113199990493
20. S.N. Silva, M. Tomar, C. Paulo, B.C. Gomes, A.P. Azevedo, V. Teixeira, J.E. Pina, J. Rueff, J.F. Gaspar, Breast cancer risk and common single nucleotide polymorphisms in homologous recombination DNA repair pathway genes XRCC2, XRCC3, NBS1 and RAD51. Cancer Epidemiol. (2010). doi:10.1016/j.canep.2009.11.002
21. R.H. Wilting, J.H. Dannenberg, Epigenetic mechanisms in tumorigenesis, tumor cell heterogeneity and drug resistance. Drug Resist. Updat (2012). doi:10.1016/j.drup.2012.01.008
22. J. Rueff, A.S. Rodrigues, Cancer Drug Resistance: A Brief Overview from a Genetic Viewpoint. Methods Mol. Biol. (2016). doi:10.1007/978-1-4939-3347-1_1
23. Y. Niu, A. Wan, Z. Lin, X. Lu, G. Wan, N6-Methyladenosine modification: a novel pharmacological target for anti-cancer drug development. Acta Pharm Sin B. doi:10.1016/j.apsb.2018.06.001
24. Q. Cui, H. Shi, P. Ye, L. Li, Q. Qu, G. Sun, G. Sun, Z. Lu, Y. Huang, C.G. Yang, A.D. Riggs, C. He, Y. Shi, m^6A RNA Methylation Regulates the Self-Renewal and Tumorigenesis of Glioblastoma Stem Cells. Cell. Rep. (2017). doi:10.1016/j.celrep.2017.02.059
25. J. Liu, M.A. Eckert, B.T. Harada, S.M. Liu, Z. Lu, K. Yu, S.M. Tienda, A. Chryplewicz, A.C. Zhu, Y. Yang, J.T. Huang, S.M. Chen, Z.G. Xu, X.H. Leng, X.C. Yu, J. Cao, Z. Zhang, J. Liu, E. Lengyel, C. He, m^6A mRNA methylation regulates AKT activity to promote the proliferation and tumorigenicity of endometrial cancer. Nat. Cell. Biol. (2018). doi:10.1038/s41556-018-0174-4
26. Q. Lan, P.Y. Liu, J.L. Bell, J.Y. Wang, S. Hüttelmaier, X.D. Zhang, L. Zhang, T. Liu, The Emerging Roles of RNA m^6A Methylation and Demethylation as Critical Regulators of Tumorigenesis, Drug Sensitivity, and Resistance. Cancer Res. (2021). doi:10.1158/0008-5472.can-20-4107
27. S. Liu, Q. Li, G. Li, Q. Zhang, L. Zhuo, X. Han, M. Zhang, X. Chen, T. Pan, L. Yan, T. Jin, J. Wang, Q. Lv, X. Sui, T. Xie, The mechanism of m^6A methyltransferase METTL3-mediated autophagy in reversing gefitinib resistance in NSCLC cells by β-elemene. Cell. Death Dis. (2020). doi:10.1038/s41419-020-03148-8
28. Z. Lin, Y. Niu, A. Wan, D. Chen, H. Liang, X. Chen, L. Sun, S. Zhan, L. Chen, C. Cheng, X. Zhang, X. Bu, W. He, G. Wan, RNA m^6A methylation regulates sorafenib resistance in liver cancer through FOXO3-mediated autophagy. EMBO J. (2020). doi:10.15252/embj.2019103181
29. L. Liu, Y. Wu, Q. Li, J. Liang, Q. He, L. Zhao, J. Chen, M. Cheng, Z. Huang, H. Ren, J. Chen, L. Peng, F. Gao, D. Chen, A. Wang, METTL3 Promotes Tumorigenesis and Metastasis through BMI1 m^6A Methylation in Oral Squamous Cell Carcinoma. Mol. Ther. (2020). doi:10.1016/j.ymthe.2020.06.024
30. D. Jin, J. Guo, Y. Wu, J. Du, L. Yang, X. Wang, W. Di, B. Hu, J. An, L. Kong, L. Pan, G. Su, m^6A mRNA methylation initiated by METTL3 directly promotes YAP translation and increases YAP activity by

regulating the MALAT1-miR-1914-3p-YAP axis to induce NSCLC drug resistance and metastasis. J. Hematol. Oncol. (2019). doi:10.1186/s13045-019-0830-6

31. M.B. Uddin, K.R. Roy, S.B. Hosain, S.K. Khiste, R.A. Hill, S.D. Jois, Y. Zhao, A.J. Tackett, Y.Y. Liu, An N6-methyladenosine at the transited codon 273 of p53 pre-mRNA promotes the expression of R273H mutant protein and drug resistance of cancer cells. Biochem. pharmacol. (2019). doi:10.1016/j.bcp.2018.12.014
32. S. Narayanan, C.Y. Cai, Y.G. Assaraf, H.Q. Guo, Q. Cui, L. Wei, J.J. Huang, C.R. Ashby Jr., Z.S. Chen, Targeting the ubiquitin-proteasome pathway to overcome anti-cancer drug resistance. Drug Resist. Updat (2020). doi:10.1016/j.drup.2019.100663
33. K. Taketo, M. Konno, A. Asai, J. Koseki, M. Toratani, T. Satoh, Y. Doki, M. Mori, H. Ishii, K. Ogawa, The epitranscriptome m^6A writer METTL3 promotes chemo- and radioresistance in pancreatic cancer cells. Int. J. Oncol. (2018). doi:10.3892/ijo.2017.4219
34. D. Dominissini, S. Moshitch-Moshkovitz, M. Salmon-Divon, N. Amariglio, G. Rechavi, Transcriptome-wide mapping of N6-methyladenosine by m^6A-seq based on immunocapturing and massively parallel sequencing. Nat. Protoc. (2013). doi:10.1038/nprot.2012.148
35. A. Weckx, K.J. Grochau, A. Grandoch, T. Backhaus, J.E. Zöller, M. Kreppel, Survival outcomes after surgical treatment of oral squamous cell carcinoma. Oral Dis. (2020). doi:10.1111/odi.13422
36. J. Lu, H. Zhong, T. Chu, X. Zhang, R. Li, J. Sun, R. Zhong, Y. Yang, M.S. Alam, Y. Lou, J. Xu, Y. Zhang, J. Wu, X. Li, X. Zhao, K. Li, L. Lu, B. Han, Role of anlotinib-induced CCL2 decrease in anti-angiogenesis and response prediction for nonsmall cell lung cancer therapy. Eur. Respir J. (2019). doi:10.1183/13993003.01562-2018
37. X.Z. Chen, Anlotinib for Refractory Advanced Non-Small Cell Lung Cancer in China. JAMA Oncol. (2019). doi:10.1001/jamaoncol.2018.5526
38. A.P. Zhou, Y. Bai, Y. Song, H. Luo, X.B. Ren, X. Wang, B. Shi, C. Fu, Y. Cheng, J. Liu, S. Qin, J. Li, H. Li, X. Bai, D. Ye, J. Wang, J. Ma, Anlotinib Versus Sunitinib as First-Line Treatment for Metastatic Renal Cell Carcinoma: A Randomized Phase II Clinical Trial. Oncologist (2019). doi:10.1634/theoncologist.2018-0839
39. Q. Yang, L. Ni, S. Imani, Z. Xiang, R. Hai, R. Ding, S. Fu, J.B. Wu, Q. Wen, Anlotinib Suppresses Colorectal Cancer Proliferation and Angiogenesis via Inhibition of AKT/ERK Signaling Cascade. Cancer Manag Res (2020). doi:10.2147/cmar.s252181
40. F. Gao, Q. Wang, C. Zhang, C. Zhang, T. Qu, J. Zhang, J. Wei, R. Guo, RNA methyltransferase METTL3 induces intrinsic resistance to gefitinib by combining with MET to regulate PI3K/AKT pathway in lung adenocarcinoma. J. Cell. Mol. Med. (2021). doi:10.1111/jcmm.16114
41. X. Bi, X. Lv, D. Liu, H. Guo, G. Yao, L. Wang, X. Liang, Y. Yang, METTL3-mediated maturation of miR-126-5p promotes ovarian cancer progression via PTEN-mediated PI3K/Akt/mTOR pathway. Cancer Gene Ther (2021). doi:10.1038/s41417-020-00222-3
42. F. Yan, A. Al-Kali, Z. Zhang, J. Liu, J. Pang, N. Zhao, C. He, M.R. Litzow, S. Liu, A dynamic N6-methyladenosine methylome regulates intrinsic and acquired resistance to tyrosine kinase inhibitors. Cell Res. doi:10.1038/s41422-018-0097-4

43. Z. Ianniello, M. Sorci, L. Ceci Ginistrelli, A. Iaiza, M. Marchioni, C. Tito, E. Capuano, S. Masciarelli, T. Ottone, C. Attrotto, M. Rizzo, L. Franceschini, S. de Pretis, M.T. Voso, M. Pelizzola, F. Fazi, A. Fatica. New insight into the catalytic-dependent and -independent roles of METTL3 in sustaining aberrant translation in chronic myeloid leukemia. Cell. Death Dis. (2021). doi:10.1038/s41419-021-04169-7

44. R. Sa, R. Liang, X. Qiu, Z. He, Z. Liu, L. Chen, IGF2BP2-dependent activation of ERBB2 signaling contributes to acquired resistance to tyrosine kinase inhibitor in differentiation therapy of radioiodine-refractory papillary thyroid cancer. Cancer Lett. (2021). doi:10.1016/j.canlet.2021.12.005

Figures

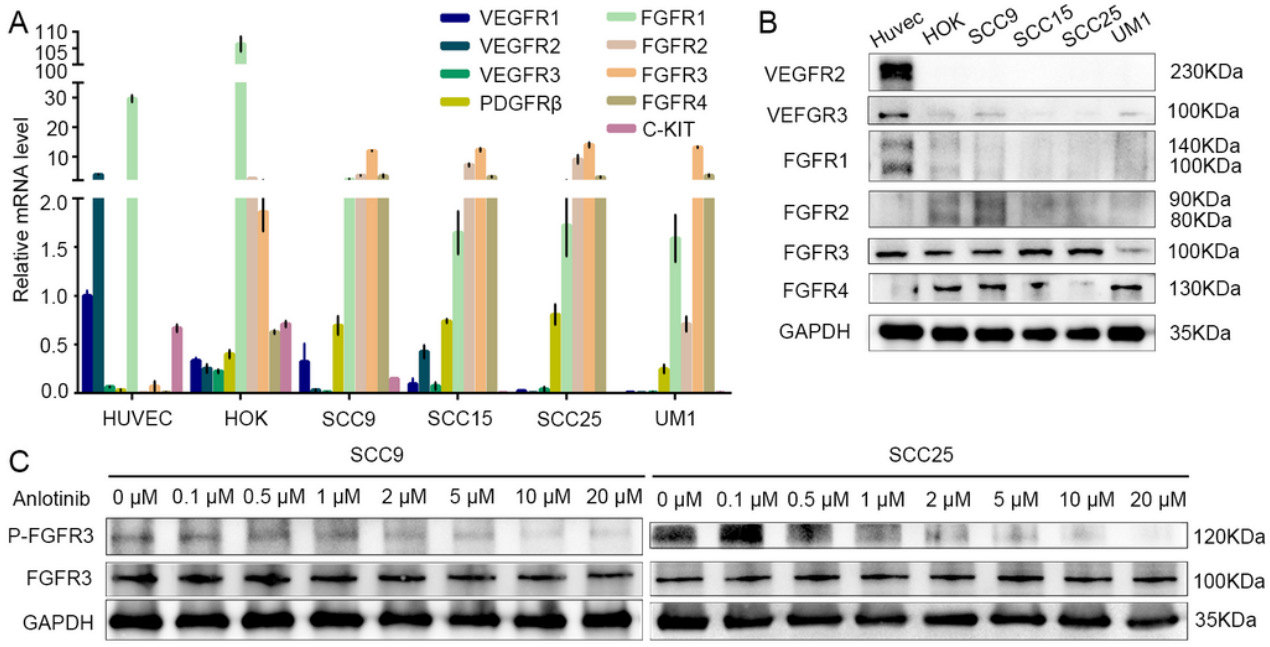

Figure 1

Anlotinib targets FGFR3 and inhibits FGFR3 phosphorylation in OSCC.

A and B. The tyrosine kinase inhibitor (TKI) targets of anlotinib were assessed by quantitative real-time PCR (qRT-PCR) and western blotting.

C. The expression and phosphorylation levels of FGFR3 were detected in concentration gradient anlotinib treated in SCC9 and SCC25 cells using the western blotting. $P < 0.05$; $^{**}P < 0.01$; $^{***}P < 0.001$.

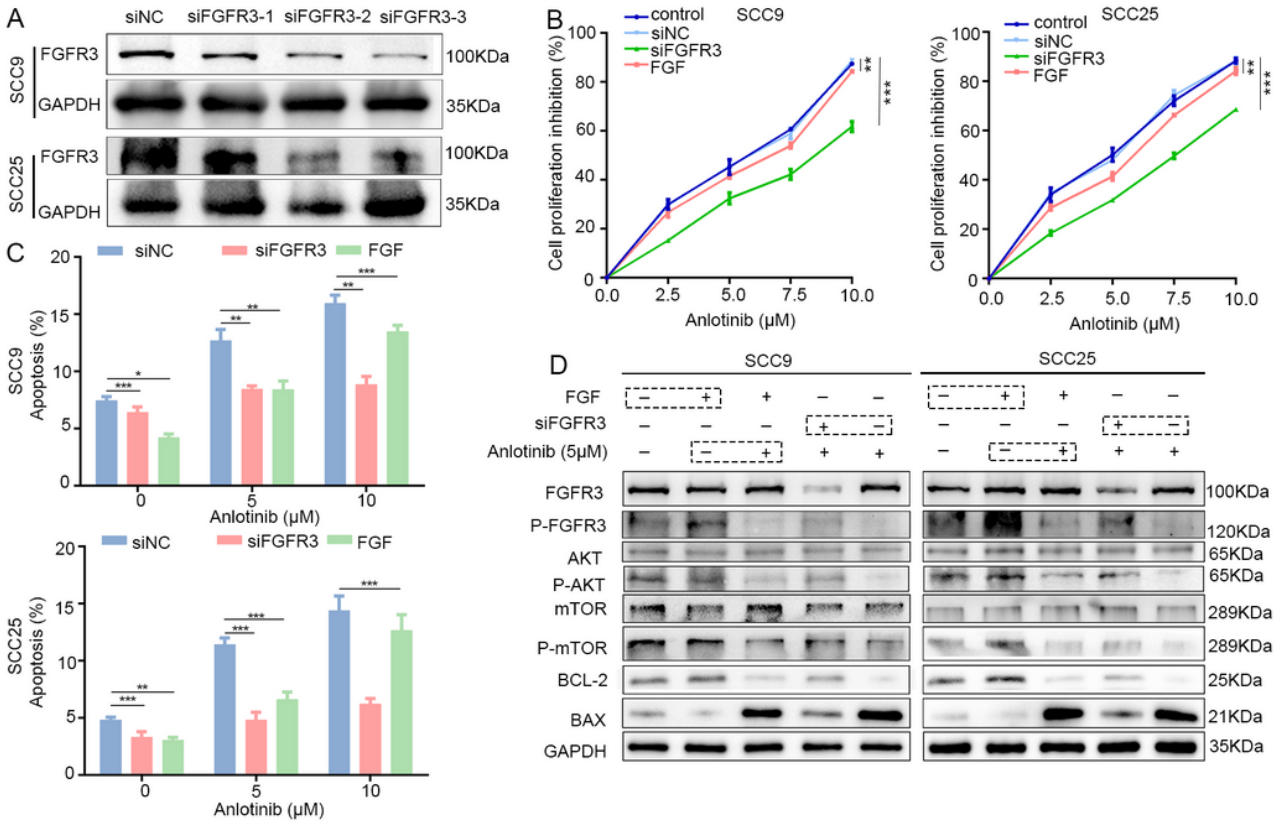

Figure 2

FGFR3 expression level affects antitumor activity of anlotinib in OSCC.

A. FGFR3 silenced effects were examined by western blotting.

B. Cell proliferation inhibition assay showed that the cytotoxic ability of anlotinib in OSCC cells (24h) after transfected with siFGFR3 or treated with rhFGF.

C. Cell apoptosis assay showed the ratio of apoptosis cells of anlotinib-treated (24h) OSCC cells after transfected with siFGFR3 or treated with rhFGF.

D. Western blotting was used to detect the expression of protein and phosphorylated protein of FGFR3, AKT and mTOR and apoptosis-related proteins in indicated treatment OSCC cells. *$P < 0.05$; **$P < 0.01$; ***$P < 0.001$.

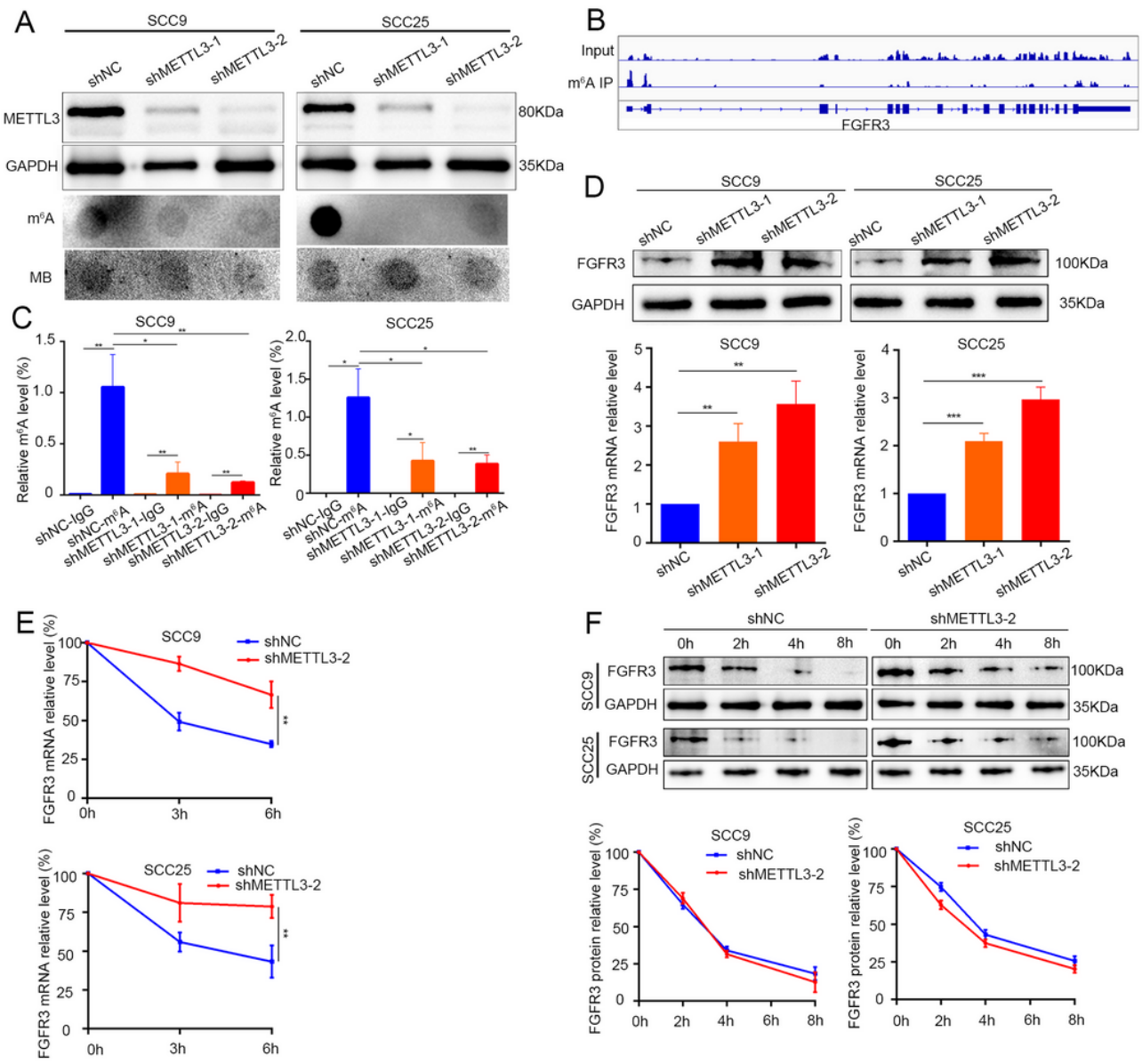

Figure 3

METTL3 regulates FGFR3 mRNA m^{6}A modification and inhibits FGFR3 mRNA stability.

A. The METTL3 protein level and m^{6}A level of RNA were detected by western blotting or dot blot in METTL3-knockdown OSCC cells (SCC9 and SCC25).

B. Representative m^{6}A modification of FGFR3 in OSCC by MeRIP-seq (data from our previous study).

C. MeRIP-qPCR showed that relative FGFR3 m^{6}A level was significantly decreased after METTL3 knockdown in SCC9 and SCC25 cells.

D. The FGFR3 protein and mRNA levels were significantly increased in METTL3 knockdown OSCC cells (SCC9 and SCC25).

E. FGFR3 mRNA stability was significantly decreased in METTL3-knockdown OSCC cells after treated with actinomycin D.

F. FGFR protein stability was no significant changes between control cells and METTL3-knockdown OSCC cells by cycloheximide assay. Quantification of the protein optical density by ImageJ. *P< 0.05; **P< 0.01; ***P< 0.001.

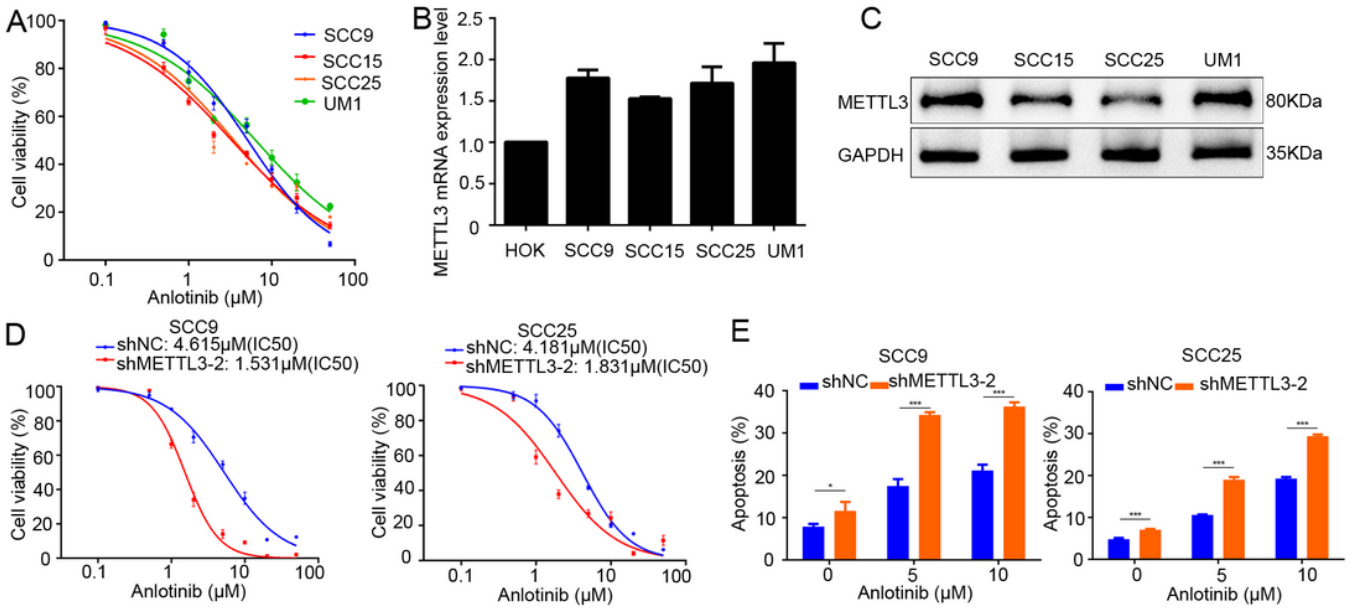

Figure 4

Levels of METTL3 are inversely associated with anlotinib sensitivity in OSCC cells.

A. The cytotoxic effect of anlotinib in different OSCC cell lines using cell viability assay.

B and C. The mRNA and protein levels of METTL3 in different OSCC cell lines using qRT-PCR and western blotting.

D. Cell viability assay showed the cytotoxic ability of anlotinib was significantly increased (decreased of IC50) in METTL3-knockdown OSCC cells compared with control cells (24h).

E. Cell apoptosis assay showed the ratio of apoptosis cells in anlotinib-treated (24h) cells was significantly increased after METTL3 knockdown in SCC9 and SCC25 cells lines. *P< 0.05; **P< 0.01; ***P< 0.001.

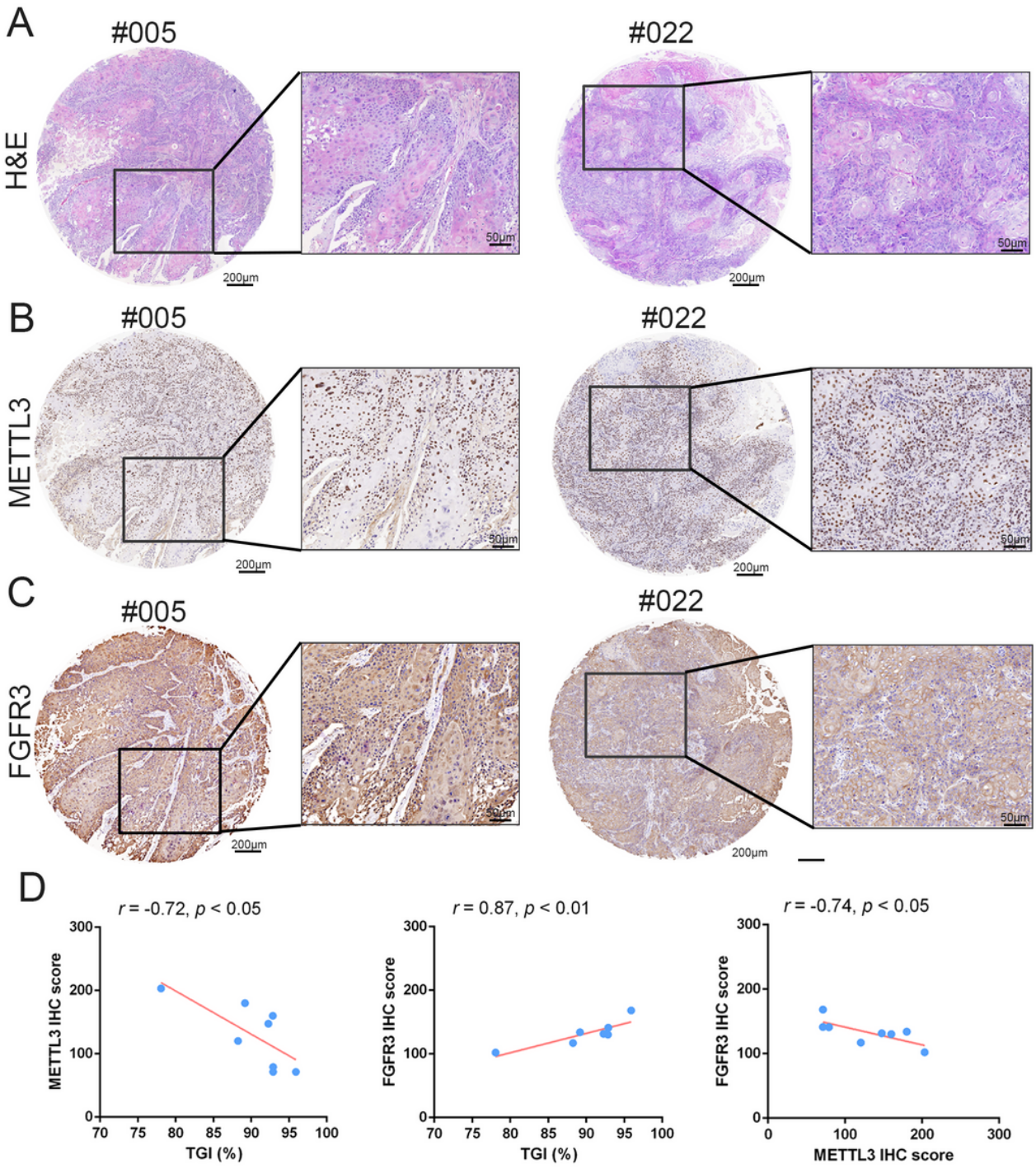

Figure 5

METTL3 affects the FGFR3 expression and antitumor efficacy of anlotinib in PDX models.

A-C. Representative H&E staining and IHC staining of METTL3 and FGFR3 in PDX models. #005 represented highest TGI rate (95.9%); #022 represented lowest TGI rate (78.07%).

D. The correlation between the IHC score of METTL3 and TGI rate, IHC score of FGFR3 and TGI rate, IHC score of METTL3 and FGFR3.

Supplementary Files

This is a list of supplementary files associated with this preprint. Click to download.

- SupplementaryFig1.tif
- SupplementaryFig2.tif
- SupplementaryFig3.tif
- TableS1.docx